
**Liquid Crystals**
Publication details, including instructions for authors and subscription information:
http://www.informaworld.com/smpp/title~content=t713926090

# A note on observability of fluctuation-induced structural interaction in a nematic mesophase

P. Ziherl; I. Muevi

Online publication date: 06 August 2010

**To cite this Article** Ziherl, P. and Muevi, I.(2001) 'A note on observability of fluctuation-induced structural interaction in a nematic mesophase', Liquid Crystals, 28: 7, 1057 — 1062
**To link to this Article: DOI:** 10.1080/02678290110048723
**URL:** http://dx.doi.org/10.1080/02678290110048723

LIQUID CRYSTALS, 2001, VOL. 28, NO. 7, 1057–1063

# A note on observability of fluctuation-induced structural interaction in a nematic mesophase

P. ZIHERL*
Department of Physics and Astronomy, University of Pennsylvania, Philadelphia, PA 19104-6396, USA

and I. MUŠEVIČ
Department of Physics, University of Ljubljana, Jadranska 19, SI-1000 Ljubljana, Slovenia

(*Received 30 October 2000; accepted 2 February 2001*)

We discuss the observability of pseudo-Casimir interaction in nematic liquid crystals, and show that in physically relevant regimes the interaction is characterized by non-universal force profiles that depend strongly on the anchoring. Depending on the ratio of the anchoring strengths, the force may be either purely attractive at all separations or it may become repulsive at separations comparable to the geometric mean of the extrapolation lengths. Within the currently accessible experimental window, it appears that the $1/h^3$ force could only be seen in very weakly anchored symmetric systems at separations no larger than a few 10 nm. We also find that while the conventional force measuring systems such as the atomic force microscope and surface force apparatus can provide some information on the fluctuation-induced force, alternative techniques, e.g. spinodal dewetting, could be used to obtain a more comprehensive insight extending over a wider range of separations.



## 1. Introduction

In 1948, Casimir discovered that the energy density of the quantum electromagnetic fluctuations in vacuum is modified by the presence of conducting plates, and that this generates a long range attractive force between the plates [1]. The idea initiated extensive theoretical studies of the effect [2] but the force proved difficult to observe experimentally. The first unambiguous measurements of the force were performed almost 50 years after the pioneering theoretical study [3, 4]. Apart from the technical difficulties, one of the main reasons for the long search for Casimir interaction is that in any real material, there are a number of corrections to the power-law force profile derived by Casimir. An important correction is due to the finite conductivity of real metals, which implies that they are transparent rather than impenetrable for electromagnetic waves beyond the plasma frequency. At distances smaller than or comparable to the wavelength corresponding to the plasma frequency, the zero-frequency boundary conditions $E_{\parallel} = B_{\perp} = 0$, which were used in the original analysis of the effect [1], are completely inadequate.

*Author for correspondence; e-mail: primoz@physics.upenn.edu; permanent address: J. Stefan Institute, Slovenia.

Similar non-idealities also occur in classical systems, where a thermal analogue of the Casimir effect is induced by fluctuations of the appropriate order parameter. In liquid crystals (LCs), director fluctuations give rise to force proportional to $1/h^3$, where $h$ is the separation between the substrates [5]. This result was derived within the limit of infinitely strong anchoring where the fluctuations are assumed to vanish at the substrates. However, in real systems the surface interaction is not infinitely strong and the fluctuation-induced force is no longer described by the universal $1/h^3$ law. It has been shown that in the case of identical substrates, the deviation from the power-law behaviour is largest at separations comparable to the length that characterizes the strength of the surface interaction [6]. This happens to be within the range of typical separations at which the force can be measured.

The situation is expected to be even more complicated in systems bounded by dissimilar substrates. This more general framework covers not only some of the standard force measurement techniques such as atomic force microscope but also spinodal dewetting [7, 8], an alternative set-up with several advantages compared with the conventional force apparatuses. In this experiment, a thin layer of liquid is spread on a solid substrate,

*Liquid Crystals* ISSN 0267-8292 print/ISSN 1366-5855 online © 2001 Taylor & Francis Ltd
http://www.tandf.co.uk/journals
DOI: 10.1080/02678290110048723

usually by spin-casting. If the derivative of force between the solid–liquid and the liquid–air interfaces with respect to film thickness is positive, the film will spontaneously disintegrate into an array of droplets [9]. By measuring the size of the droplets and the dewetting time as a function of the initial thickness of the film, one could reconstruct the profile of the interaction between the interfaces.

There are some indications that the fluctuation-induced interaction in LCs could be studied systematically with existing experimental techniques [10], and the aim of this paper is to facilitate future experiments by analysing the behaviour of the force in nematic liquid crystals (NLCs) within the physically relevant range of material parameters and experimentally accessible separations. In other words, we will determine how this interaction should appear within the experimental windows of the different techniques. In § 2, we summarize the theory of the fluctuation-induced force in nematic liquid crystals and present the reduced force amplitudes for different relative anchoring strengths. We show that in the case of dissimilar substrates, the force departs from the $1/h^3$ law much more dramatically than in a system with identical substrates. In § 3 we estimate the experimentally accessible ranges of separations and surface anchoring strengths, and discuss the force profiles within this context. We also analyse the pros and cons of the different experimental techniques and give a few guidelines as to what systems are most suitable for a particular technique. Section 4 concludes the paper.



## 2. Fluctuation-induced force

The pseudo-Casimir force in NLCs has been already studied theoretically in some detail, and most [5, 6, 11] though not all [12] studies deal with the phenomenon in planar geometry. Unless one intends to study how the amplitude of the fluctuation-induced force depends on the shapes of the interacting bodies, there are two good reasons for choosing planar geometry. First, it is rather transparent from the theoretical viewpoint, which is convenient when discussing effects not related to the specific geometry; second, it covers the most widely used liquid-crystalline experimental set-up. At the same time, these results can be transplanted to non-planar systems as long as the director fields in the two geometries are identical: the force between two curved surfaces is related to the interaction between parallel plates by the Derjaguin approximation [13].

For these reasons, we limit the analysis to a planar model system consisting of a nematic film bounded by two solid substrates or, alternatively, by a solid substrate and air. We assume that the preferred molecular orientations at the two interfaces, located at $z = \pm h/2$, are identical but the anchoring strengths $W_1$ and $W_2$, are different. In this case, the equilibrium director field is uniform at all separations and there is no mean-field interaction between the interfaces.

### 2.1. *Interaction free energy*

Similar systems have been discussed in related contexts [5, 6, 11] and here we will merely sketch the theory based on the one-constant Frank elastic energy and Rapini–Papoular surface interaction. We assume that the anchoring is non-degenerate, say homeotropic; then the Hamiltonian of the system is given by

$$H[\mathbf{n}] = \frac{K}{2}\left\{\int\left[(\nabla \cdot \mathbf{n})^2 + (\nabla \times \mathbf{n})^2\right] \mathrm{d}V - \lambda_1^{-1}\int (\mathbf{n} \cdot \mathbf{e}_z)^2\, \mathrm{d}S_1 - \lambda_2^{-1}\int (\mathbf{n} \cdot \mathbf{e}_z)^2\, \mathrm{d}S_2\right\} \quad (1)$$

where $K$ is the elastic constant; $\mathbf{n} = \mathbf{n}(\mathbf{r})$ is the nematic director subject to constraint $|\mathbf{n}| = 1$; $\lambda_i = K/W_i$, $i = 1, 2$, are the so-called extrapolation lengths; and $\mathbf{e}_z$ is the normal to the substrates. Assuming that the fluctuations are small, we can write $\mathbf{n} = n_x\mathbf{e}_x + n_y\mathbf{e}_y + (1 - n_x^2/2 - n_y^2/2)\mathbf{e}_z$, where $n_x$ and $n_y$ are the two fluctuating scalar degrees of freedom, and $\mathbf{e}_x$ and $\mathbf{e}_y$ are the in-plane components of the Cartesian triad that defines the coordinate system. Then we expand $H$ to second order

$$H[\mathbf{n}] = \frac{K}{2}\sum_{w=x,y}\left[\int (\nabla n_w)^2\, \mathrm{d}V + \lambda_1^{-1}\int n_w^2\, \mathrm{d}S_1 + \lambda_2^{-1}\int n_w^2\, \mathrm{d}S_2\right] \quad (2)$$

and the interaction free energy associated with this harmonic Hamiltonian is [11]

$$F_{\mathrm{int}} = -\frac{k_{\mathrm{B}}TS}{2\pi}\int_0^\infty \ln[1 - \Delta(q, \lambda_1, \lambda_2)\exp(-2qh)]q\, \mathrm{d}q. \quad (3)$$

Here $k_{\mathrm{B}}$ is the Boltzmann constant, $T$ is temperature, $S$ is the area of the substrates,

$$\Delta(q, \lambda_1, \lambda_2) = \left(\frac{q - \lambda_1^{-1}}{q + \lambda_1^{-1}}\right)\left(\frac{q - \lambda_2^{-1}}{q + \lambda_2^{-1}}\right) \quad (4)$$

and $q$ is the magnitude of the in-plane modulation of the fluctuations $q = q_x\mathbf{e}_x + q_y\mathbf{e}_y$.

### 2.2. *Reduced amplitude*

The system is characterized by three lengthscales, $h$, $\lambda_1$, and $\lambda_2$, and its behaviour depends on the ratios of extrapolation lengths and the thickness. If $\lambda_1/h$ is large, the restoring torque at the wall 1 is small and the anchoring is effectively weak at $z = -h/2$. In the limit $\lambda_1/h \to \infty$, the fluctuations are subjected to Neumann boundary conditions, $dn_w/dz(z = -h/2) = 0$. In the opposite case where $\lambda_1/h$ is small, the fluctuations are suppressed at the wall and the anchoring is said to be strong. For $\lambda_1/h \to 0$ the boundary conditions are of Dirichlet type: $n_w(z = -h/2) = 0$. The same applies to wall 2.

The idealized examples where the extrapolation lengths are either infinitely large or infinitely small were discussed in the first theoretical study of the pseudo-Casimir effect in LCs [5]. In the case of zero anchoring strength at both substrates (Neumann–Neumann boundary conditions), the fluctuation-induced force between the substrates is attractive

$$\mathcal{F}_{\text{int}}(\lambda_1 \to \infty, \lambda_2 \to \infty, h) = -\frac{\zeta(3)k_B T S}{8\pi h^3}. \tag{5}$$

The functional part of the force, $k_B T S/h^3$, can be predicted by dimensional arguments, whereas its amplitude is determined by the boundary conditions. Infinitely strong anchoring at one wall and zero anchoring at the other (mixed, Dirichlet–Neumann boundary conditions) induce a repulsive force with a somewhat smaller amplitude:

$$\mathcal{F}_{\text{int}}(\lambda_1 = 0, \lambda_2 \to \infty, h) = \frac{3\zeta(3)k_B T S}{32\pi h^3}. \tag{6}$$

The relative strength of the force can be expressed conveniently by the reduced amplitude defined relative to the amplitude of the force in a symmetric system with infinitely weak anchoring

$$\rho = \frac{\mathcal{F}_{\text{int}}(\lambda_1, \lambda_2, h)}{\mathcal{F}_{\text{int}}(\lambda_1 \to \infty, \lambda_2 \to \infty, h)}. \tag{7}$$

The reduced amplitude for mixed boundary conditions is therefore $-3/4$. Finally, in the case of infinitely strong anchoring at both substrates (Dirchlet–Dirchlet boundary conditions) the force is again given by equation (5). This is not really surprising, because the spectrum of fluctuations is the same as for Neumann–Neumann boundary conditions although the symmetry of the normal modes is different [6].

The three limiting cases illustrate a well known property of the fluctuation-induced interaction: in systems with symmetric anchoring, either infinitely weak or infinitely strong, the force is attractive, whereas in systems with mixed anchoring the force is repulsive. As we will show, the rigorous notions of 'symmetric' and 'mixed' boundary conditions should be relaxed to 'similar' and 'dissimilar' boundary conditions.

Within the idealized, zero-parametric models of surface interaction, the three force regimes are completely unrelated. But within the more realistic boundary conditions they follow naturally one after another as the separation of the plates is varied; moreover, the transitions between them are continuous. This is rather easy to understand. If the separation of the walls is much smaller than both extrapolation lengths, $h \ll \lambda_1, \lambda_2$, the effective anchoring at the substrates is weak yet non-zero (figure 1). The system is characterized by weak boundary conditions with finite but small derivative of the normal modes at both substrates (as opposed to purely Neumann boundary conditions with zero derivative). Although the boundary conditions are similar rather than identical, the system is qualitatively symmetric and the force is attractive. At somewhat larger distances, $h$ is larger than the smaller extrapolation length ($h > \lambda_1$) yet smaller than the large one ($h < \lambda_2$). The boundary condition at wall 1 is strong with small yet non-zero magnitude of fluctuations and weak at wall 2. In this case, the boundary conditions are dissimilar and the force is repulsive. At large distances, where the separation is larger than both extrapolation lengths, $h > \lambda_1, \lambda_2$, both anchorings become effectively strong, and the force is attractive again.

A quantitative analysis of the reduced amplitude (i.e. the ratio of the actual and either small- or large-$h$ amplitudes) of the fluctuation-induced force is shown in figure 2. The separation between the substrates is scaled by the geometric mean of the extrapolation lengths

$$\Lambda = (\lambda_1 \lambda_2)^{1/2} \tag{8}$$

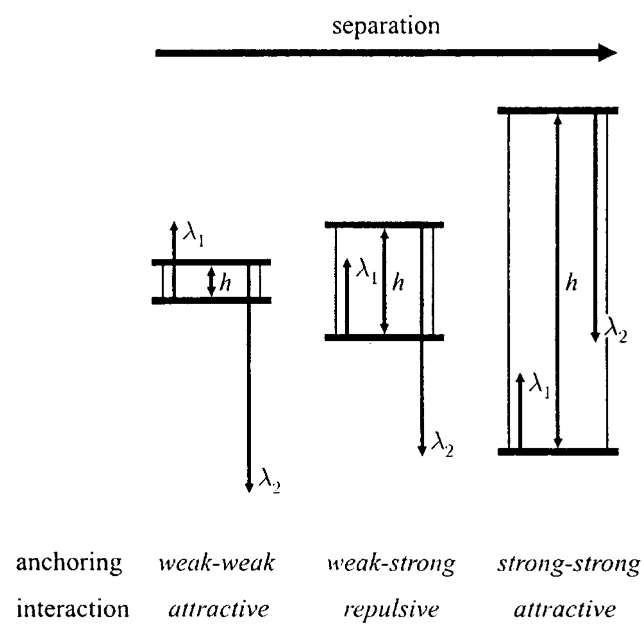


Figure 1. An illustration of the continuous transformation of the small-separation regime with weak–weak anchoring, to the intermediate-separation regime with weak–strong anchoring, and then to the large-separation regime with strong–strong anchoring.

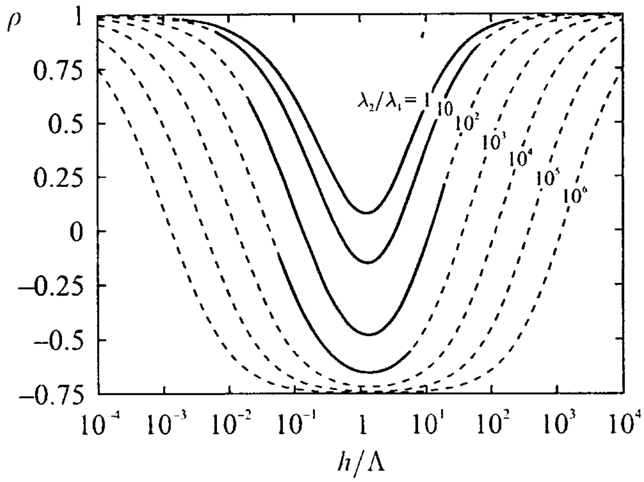


Figure 2. Reduced amplitude of the fluctuation-induced force as a function of the reduced distance for $\lambda_2/\lambda_1 = 1$, 10, $10^2$, $10^3$, $10^4$, $10^5$, and $10^6$. At large $\lambda_2/\lambda_1$, the intermediate-separation regime is well developed, and the reduced amplitude approaches $-3/4$ over several orders of magnitude. At small $\lambda_2/\lambda_1$ the transition from small-separation to large-separation regimes is direct. The solid segments of the curves are the observable regimes as described in § 3.



and the different curves are labelled by their ratio, $\lambda_2/\lambda_1$. In the case of very dissimilar extrapolation lengths—say for $\lambda_2/\lambda_1 \gtrsim 10^6$—the intermediate-separation repulsive regime is fully developed and the reduced amplitude is quite close to $-3/4$ for reduced separations extending over more than two orders of magnitude. Also note that the transition from the intermediate-separation to either small- and large-separation regimes is rather broad; it extends over about three orders of magnitude. At smaller $\lambda_2/\lambda_1$, the repulsive regime is less pronounced and the reduced amplitude does not level off at any given value, which means that the force profile will not obey the $1/h^3$ law at intermediate separations. At $\lambda_2/\lambda_1 \lesssim 3.5$, the repulsive regime vanishes altogether and the force is attractive at all separations. In this case, the dip in the reduced amplitude of the force is nothing but a remnant of the absent intermediate-separation repulsive regime that separates the small-$h$ attraction characterized by weak–weak anchoring from the large-separation attraction characterized by strong–strong anchoring.

Finally, let us briefly describe the fluctuation-induced force in a related yet somewhat different system where the easy axes do not coincide. In this case, the director would be uniform only at distances smaller than the critical separation $h_c = |\lambda_1 - \lambda_2|$ [14], whereas at large separations the director is distorted, which implies that the fluctuation-induced effects are obscured by the mean-field elastic interaction. The structural force in the uniform configuration has been discussed in some detail recently [10, 11], and it shares many features with the system studied in this paper. The main difference is that the large-separation attractive regime is always absent because the system undergoes a structural transition before reaching it. On the other hand, the intermediate-separation repulsive regime may be present if the anchoring strengths are not too similar. But as we will see, the large-separation regime is largely irrelevant from the experimental point of view, so that the observable fluctuation-induced force should not really depend on the relative orientation of the easy axes.

## 3. Discussion

### 3.1. *Length-scales*

To determine the physically relevant and experimentally accessible sections of the force-separation diagram, we must find the realistic ranges of the three lengths involved. The lower limit of the separation of the substrates is determined by the molecular size—a few nm—and it tells us when the system starts to behave as a continuum. On the other hand, the upper limit depends on the sensitivity of the force apparatus. Measurements of the structural force are usually performed using the surface force apparatus (SFA) [15, 16] or atomic force microscope (AFM) [17, 18], which use crossed cylinders and sphere–plane arrangement, respectively. Provided that the director field is uniform, the total force in these curved geometries is given by the Derjaguin approximation

$$\mathscr{F} = \frac{2\pi R}{S} F_{\text{int}} \tag{9}$$

where $R$ is the radius of the two cylinders in SFA (which are assumed to be identical and at right angles) or the sphere in AFM experiment, and $F_{\text{int}}$ is the interaction free energy for flat substrates [13]. In a typical SFA, $R \approx 20$ mm [16, 19] and the force sensitivity of the apparatus, $\mathscr{F}_N$, is about 10 nN [13, 16]. This means that this apparatus is precise enough to detect the fluctuation-induced force [see equation (5)] at distances up to $\approx 40$ nm, which is not much. Unfortunately, AFM is no better. Its force sensitivity is determined primarily by the noise due to Brownian motion of the microsphere glued on the cantilever of the microscope and is considerably better, around 10 pN. But the radius of curvature of the sphere is also much smaller. Usually, it is no larger than about 20 μm, which gives an essentially identical figure of merit $\mathscr{F}_N/R$.

In spinodal dewetting experiments, the upper limit of separation of the substrates $h$ depends on the stability of the liquid film. At large thicknesses, the dewetting times may become very long and thus hard to estimate accurately, or else the film can be unstable and rupture via another dewetting mechanism such as nucleation of holes. In this case, the determination of the upper limit of the separation is neither trivial nor very general, but it has been shown empirically that it can reach about 100 nm [20] which is more than twice as much as in SFA and AFM. Since we intend to determine the limits of observability within an order of magnitude, we conclude that the experimentally relevant range of $h$ is from 1 to 100 nm.

The range of extrapolation lengths, $\lambda_i = K/W_i$, is somewhat larger. The elastic constant typically varies between 1 pN and 10 pN [21] and is temperature-dependent. The anchoring strength depends on the LC, substrate and its treatment, and temperature. It can vary from about $1\,\mu J\,m^{-2}$ to a few $mJ\,m^{-2}$ [22], so that the physically relevant range of $\lambda$ values is from a few nm to a few μm. In other words: in any LC compound, the ratio of extrapolation lengths cannot exceed $10^3$, implying that the intermediate-separation repulsive regime cannot fully develop. While we can expect that the fluctuation-induced force in some nematic systems will be repulsive for $h$ values ranging over up to 3 orders of magnitude, it should not follow the simple $1/h^3$ law. Instead, the force profile is a more complicated function of separation as described by the reduced amplitudes shown in figure 2.

Given the above limits for the extrapolation lengths and separation of the substrates, we can distinguish between three extremes:

(1) In systems with as dissimilar anchoring strengths as possible, where $\lambda_2/\lambda_1 = 10^3$, $\Lambda$ is a few 10 nm, so that $h/\Lambda$ varies from 0.1 to 10. In this range, the fluctuation-induced force is purely repulsive.
(2) In the case of identical substrates with rather strong anchoring, $\Lambda \sim 1$ nm and $h/\Lambda$ goes from 1 to 100, which corresponds to an attractive force that decays more slowly than $1/h^3$. In fact, the force profile is not very different from a $1/h^2$-law for $h/\Lambda$ values between 1 and 10, whereas for $h/\Lambda$ values from 10 to 100 the force profile approaches $1/h^3$.
(3) If the anchoring is very weak rather than very strong (the substrates still being identical) $\Lambda$ is of the order of 1 μm and $h/\Lambda$ ranges from 0.001 to 0.1. In this case, the force decays almost as $1/h^3$ at small $h$.

The parameters of these extreme situations actually determine the relevant range of force-measuring experiments for the fluctuation-induced force in NLCs as depicted in figure 2. (Of course, the actual limits of observability are not as sharp as shown in the figure.)

Clearly, the observable pseudo-Casimir force in nematics obeys the universal $1/h^3$ power law only in very weakly anchored symmetric systems; the universal behaviour is to be expected at small distances where the fluctuation-induced force is strong. This is as close as one can get to the universal exponent of $-3$ in any nematic system. In principle, one could approach the same power law in thick strongly-anchored symmetric systems as well, but in this case the force would be rather weak and not as easy to extract from the data. In all other cases, the transitional regime with non-algebraic force profile that may also be non-monotonic and change from attraction to repulsion (and back) is expected. Within the narrow experimental window of intersubstrate separation, which may span as little as one but rarely more than two orders of magnitude, this non-universal behaviour could be misidentified as a power law with an exponent other than 3.

Although they may appear restrictive enough, the limitations discussed so far are not the only ones. There are three additional experimental issues that have to be taken into account: mechanical (in)stability of set-ups, non-pseudo-Casimir structural forces, and non-structural forces. As we will see, these issues largely determine the suitability of a particular technique for studies of the fluctuation-induced force. We address these points in the following paragraphs.

### 3.2. *Mechanical stability*

The force measurement apparatuses can probe only certain segments of the total force profile, not the whole of it. The reason for this is that in SFA and AFM one of the interacting surfaces is suspended on a spring of stiffness $k$, and the system is mechanically unstable whenever the derivative of the force with respect to separation is larger than $k$. Typically $k$ is quite small so that the stability condition can be approximated by $d\mathcal{F}/dh < 0$, where $\mathcal{F}$ is the force between the interacting surfaces. This implies that we can only access the force at separations where the total force between flat surfaces is repulsive. However, in the improved version of the standard SFA, the so-called force feedback surface force apparatus, the cantilever instability can be reduced considerably, thereby making the attractive sections of the force profile partly accessible to measurement [23].

In spinodal dewetting, a similar restriction is based on the dewetting condition. This technique can provide information on the derivative of the force only if the film is unstable and dewets, and the dewetting condition is that this derivative be positive. One could say that in this respect, spinodal dewetting is partly complementary to SFA and AFM, because as long as the force is monotonic a positive derivative of the force implies that the interaction is attractive.

### 3.3. *Non-pseudo-Casimir structural forces*

The most ubiquitous source of structural interaction is the short range positional order of molecules at the wall [15, 16, 24]. This presmectic layering gives rise to a short range interaction that includes an oscillatory mean-field interaction [24] and a purely attractive fluctuation-induced interaction [25], and may be quite prominent at separations smaller than the correlation length of presmectic order, which is typically a few nm [19]. The mean-field part of the force can be important because its magnitude, determined by the degree of substrate-stabilized positional order [24], can be larger than $k_B T$. In principle, this effect is more pronounced in smectogenic materials. Another short range force that may be present is the interaction caused by enhanced orientational order at the wall [26] which depends on the aligning power of the substrate and may also screen the nematic fluctuation-induced interaction at small distances.

In spinodal dewetting experiments, these short range interactions are the only additional structural forces, provided that the easy axes at the two interfaces are identical or the film is thin enough [14]. In AFM and SFA experiments, this is not the case: the curved geometry of the apparatuses usually induces a distortion of the director field, which gives rise to a long range repulsion between the interfaces. Dimensional arguments suggest that the ratio of the fluctuation-induced interaction and the mean-field repulsion is $k_B T/Kh_0$, where $K$ is the elastic constant and $h_0$ is the characteristic length of the system, i.e. the sphere (or cylinder) radius $R$. In a typical AFM set-up, $R$ is about $10\,\mu m$ and $k_B T/Kh_0 \approx 10^{-4}$, whereas in SFA $R$ is usually $\sim 10$ mm so that this ratio is even smaller, about $10^{-7}$. This suggests that unless the mean-field force is absent, the fluctuation-induced force will play a subdominant role. It is therefore desirable to study the effect in a set-up where the director field between the interacting surfaces is uniform.

Although a detailed analysis of the director field between a sphere and a flat wall (AFM) and between two cylinders (SFA) has been carried out only in the limit of infinitely strong anchoring [27], we can still make a semiquantitative prediction as to whether or not the mean-field interaction can be avoided. We rely on a theoretical study of the director field around an isolated spherical colloidal particle suspended in a nematic matrix [28], which shows that a so-called weak anchoring regime with more or less uniform and defectless director field is stable at $R/\lambda \lesssim 10$, where $\lambda$ is the extrapolation length at the surface of the sphere. As mentioned above, $\lambda$ can reach a few μm, and in AFM $R$ is typically about $10\,\mu m$, which means that this condition can be fulfilled. Furthermore, the region of stability of the defectless configuration is extended by the presence of the wall, which acts as an additional aligning agent. We can expect that in an AFM experiment with very weak anchoring at the sphere and very strong anchoring at the wall, the mean-field elastic force could be quite small or even absent. In this case, we should expect a repulsive fluctuation-induced interaction with a non-universal force profile (figure 2, $\lambda_2/\lambda_1 \approx 10^3$).

A similar estimate for the crossed cylinders in SFA is obviously less accurate because the director field around a cylindrical inclusion in a nematic matrix has not been studied theoretically for arbitrary anchoring strength. Nevertheless, we can assume that the ratio $R/\lambda$ has basically the same meaning although its (unknown) critical value is somewhat different from that for an isolated sphere. But in SFA, $R$ is typically about 10 mm so that $R/\lambda$ is about 1000, even if the anchoring strength is extremely weak. This indicates that the SFA geometry is well within the strong anchoring regime where the director field is highly distorted and the corresponding elastic force is dominant. Another problem with SFA is that in the non-uniform regime, the Derjaguin approximation is no longer valid and a more elaborate analysis of the fluctuation-induced interaction should be carried out. SFA is therefore less appropriate for measurements of the fluctuation-induced forces in NLCs: the cylinders are simply too big.

### 3.4. *Non-structural forces*

The non-structural forces include electrostatic and polarization forces [13] such as the van der Waals force, which is long range and of the same order of magnitude as the pseudo-Casimir force. The sign and the magnitude of the van der Waals force can be controlled by adjusting the indices of refraction of the substrates and the LC (which is relatively easy in spinodal dewetting studies but not very trivial in SFA and AFM measurements). In particular, if they are very close, the van der Waals force will be greatly reduced in magnitude.

In some cases, the presence of the van der Waals background may be an advantage: for example, the attractive fluctuation-induced forces are invisible by SFA and AFM, and they can only be probed if superimposed onto a repulsive van der Waals force such that the total force is also repulsive at least for a certain range of separations. On the other hand, in a spinodal dewetting experiment an attractive van der Waals force would be desirable because it would extend the range of $h$ values where the dewetting occurs. The behaviour of the van der Waals force is well-understood theoretically [29] and one can readily subtract it from the data, thereby extracting the structural force.

## 4. Conclusions

In an effort to extend the theoretical ground for experimental studies of the pseudo-Casimir effect in nematic liquid crystals, we have analysed the fluctuation-induced force in a nematic system bounded by substrates characterized by identical easy axes but dissimilar anchoring strengths. The force profile can be divided into the attractive small-separation regime, repulsive intermediate-separation regime—which may be partly or completely suppressed if the anchoring strengths are too similar—and attractive large-separation regime. The continuous transitions between them are quite broad so that the deviations from the universal $1/h^3$ law, usually associated with the thermal analogue of the Casimir effect in correlated liquids, are absolutely essential.

Once the actual material and experimental parameters are taken into account, the non-universality of the fluctuation-induced structural force becomes even more apparent. We find that in real nematic systems, the experimentally accessible force profiles should not conform to an either attractive or repulsive $1/h^3$ law unless the anchoring is very weak at both walls. The repulsive intermediate-separation regime cannot fully develop because of the limited range of anchoring strengths, and the attractive small-separation and large-separation regimes are inaccessible because of the restricted experimental window of the different force apparatuses. Instead of the universal force profile, a more complicated and anchoring-specific behaviour is to be expected over the experimentally relevant range of separations and beyond.

This suggests that although the existing experimental techniques are sensitive enough to detect the fluctuation-induced force, the data should be analysed with some care. The various known components of the total force, such as the short range oscillatory presmectic force and the van der Waals force, should be identified properly and the remaining signal should be checked for consistency with the fluctuation-induced force for given anchoring strengths, preferably determined in an independent experiment. Last but not least, we find that while the standard force apparatuses (the atomic force microscope in particular) may provide some insight into the pseudo-Casimir effect, indirect gaugeless techniques such as spinodal dewetting are expected to probe it within a somewhat wider range of thicknesses and for a less restricted range of anchoring strengths. However, the data collected in a spinodal dewetting experiment could be less straightforward to interpret. It may well prove that the existing theory of spinodal dewetting [9] must be extended to include the non-linear effects if the observables—dewetting time and size of droplets—are to be related accurately enough to the interaction between the substrates.



We would like to thank S. Žumer, R. Podgornik, L. Bocquet, H. Stark and M. P. Valignat for stimulating discussions.

## References


[1] Casimir, H. B. G., 1948, *Proc. Kon. Ned. Akad. Wet.*, **51**, 793.

[2] For an extensive body of references see Lamoreaux, S. K., 1999, *Am. J. Phys.*, **67**, 850.

[3] Lamoreaux, S. K., 1997, *Phys. Rev. Lett.*, **78**, 5; Lamoreaux, S. K., 1998, *Phys. Rev. Lett.*, **81**, 5475(E).

[4] Mohideen, U., and Roy, A., 1998, *Phys. Rev. Lett.*, **81**, 4549.

[5] Ajdari, A., Peliti, L., and Prost, J., 1991, *Phys. Rev. Lett.*, **66**, 1481.

[6] Ziherl, P., Podgornik, R., and Žumer, S., 1998, *Chem. Phys. Lett.*, **295**, 99.

[7] Herminghaus, S., Jacobs, K., Mecke, K., Bischof, J., Fery, A., Ibn-Elhaj, M., and Schlagowski, S., 1998, *Science*, **282**, 916.

[8] Vandenbrouck, F., Valignat, M. P., and Cazabat, A. M., 1999, *Phys. Rev. Lett.*, **82**, 2693.

[9] Brochard Wyart, F., and Daillant, J., 1990, *Can. J. Phys.*, **68**, 1084.

[10] Ziherl, P., Podgornik, R., and Žumer, S., 2000, *Phys. Rev. Lett.*, **84**, 1228.

[11] Ziherl, P., Karimi Pour Haddadan, F., Podgornik, R., and Žumer, S., 2000, *Phys. Rev. E*, **61**, 5361.

[12] Bartolo, D., Long, D., and Fournier, J.-B., 2000, *Europhys. Lett.*, **49**, 729.

[13] Israelachvili, J. N., 1992, *Intermolecular and Surface Forces* (London: Academic Press).

[14] Barbero, G., and Barberi, R., 1983, *J. Phys. (Paris)*, **44**, 609.

[15] Horn, R. G., Israelachvili, J. N., and Perez, E., 1981, *J. Phys. I*, **42**, 39.

[16] Moreau, L., Richetti, P., and Barois, P., 1994, *Phys. Rev. Lett.*, **73**, 3556.

[17] Mate, C. M., Lorenz, M. R., and Novotny, V. J., 1989, *J. chem. Phys.*, **90**, 7550.

[18] Muševič, I., unpublished results.

[19] Koltover, I., Idziak, S. J. H., Davidson, P., Li, Y., Safinya, C. R., Ruths, M., Steinberg, S., and Israelachvili, J. N., 1996, *J. Phys. II Fr.*, **6**, 893.

[20] Vandenbrouck, F., Valignat, M. P., and Cazabat, A. M., unpublished results.

[21] De Gennes, P. G., and Prost, J., 1993, *The Physics of Liquid Crystals* (Oxford: Clarendon Press).

[22] Blinov, L. M., Sonin, A. Yu., and Kabayenkov, A. A., 1989, *Liq. Cryst.*, **5**, 645.

[23] Stewart, A. M., and Parker, J. L., 1992, *Rev. sci. Instrum.*, **63**, 5626.

[24] De Gennes, P. G., 1990, *Langmuir*, **6**, 1448.

[25] Ziherl, P., 2000, *Phys. Rev. E*, **61**, 4636.

[26] Poniewierski, A., and Sluckin, T. J., 1987, *Liq. Cryst.*, **2**, 281.

[27] Terentjev, E. M., 1995, *Phys. Rev. E*, **51**, 1330.

[28] Ruhwandl, R. W., and Terentjev, E. M., 1997, *Phys. Rev. E*, **56**, 5561.

[29] Mahanty, J., and Ninham, B. W., 1976, *Dispersion Forces* (London: Academic Press).